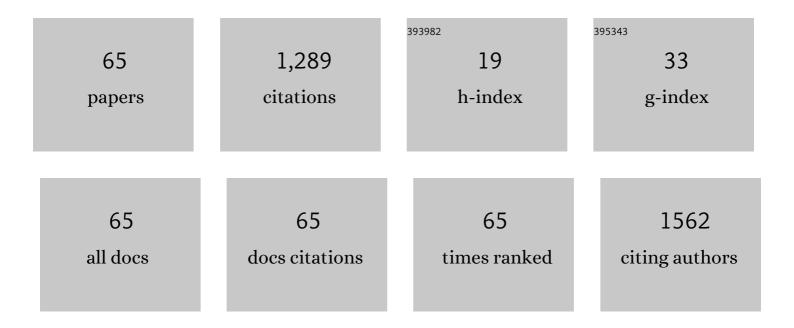
C?dric Pardanaud

List of Publications by Year in descending order

Source: https://exaly.com/author-pdf/1904151/publications.pdf Version: 2024-02-01



#	Article	IF	CITATIONS
1	A Guide to and Review of the Use of Multiwavelength Raman Spectroscopy for Characterizing Defective Aromatic Carbon Solids: from Graphene to Amorphous Carbons. Coatings, 2017, 7, 153.	1.2	272
2	Plasma–wall interaction studies within the EUROfusion consortium: progress on plasma-facing components development and qualification. Nuclear Fusion, 2017, 57, 116041.	1.6	75
3	The temperature dependence of optical properties of tungsten in the visible and near-infrared domains: an experimental and theoretical study. Journal Physics D: Applied Physics, 2017, 50, 455601.	1.3	56
4	Raman spectroscopy investigation of the H content of heated hard amorphous carbon layers. Diamond and Related Materials, 2013, 34, 100-104.	1.8	51
5	Advanced spectroscopic analyses on a:C-H materials: Revisiting the EELS characterization and its coupling with multi-wavelength Raman spectroscopy. Carbon, 2017, 112, 149-161.	5.4	51
6	Deuterium inventory in Tore Supra: Coupled carbon–deuterium balance. Journal of Nuclear Materials, 2013, 438, S120-S125.	1.3	38
7	Nuclear spin conversion of water diluted in solid argon at 4.2K: Environment and atmospheric impurities effects. Chemical Physics Letters, 2007, 447, 232-235.	1.2	35
8	Multiwavelength Raman spectroscopy analysis of a large sampling of disordered carbons extracted from the Tore Supra tokamak. Vibrational Spectroscopy, 2014, 70, 187-192.	1.2	33
9	Negative-ion production on carbon materials in hydrogen plasma: influence of the carbon hybridization state and the hydrogen content on H ^{â^'} yield. Journal Physics D: Applied Physics, 2014, 47, 085201.	1.3	32
10	Emissivity measurement of tungsten plasma facing components of the WEST tokamak. Fusion Engineering and Design, 2019, 149, 111328.	1.0	32
11	Nuclear spin conversion of H2O trapped in solid xenon at 4.2K: A new assignment of ν2 rovibrational lines. Chemical Physics Letters, 2009, 480, 82-85.	1.2	29
12	Observation of nuclear spin species conversion inside the 1593cmâ^'1 structure of H2O trapped in argon matrices: Nitrogen impurities and the H2O:N2 complex. Journal of Molecular Structure, 2008, 873, 181-190.	1.8	24
13	Enhanced negative ion yields on diamond surfaces at elevated temperatures. Journal Physics D: Applied Physics, 2011, 44, 372002.	1.3	23
14	Analysis of carbon deposited layer growth processes in Tore Supra. Journal of Nuclear Materials, 2009, 390-391, 49-52.	1.3	20
15	Analyses of dust samples collected in the MAST tokamak. Journal of Nuclear Materials, 2010, 401, 130-137.	1.3	20
16	Characterization and origin of large size dust particles produced in the Alcator C-Mod tokamak. Nuclear Materials and Energy, 2017, 11, 12-19.	0.6	20
17	Identification of BeO and BeOxDy in melted zones of the JET Be limiter tiles: Raman study using comparison with laboratory samples. Nuclear Materials and Energy, 2018, 17, 295-301.	0.6	20
18	Characterization of temperature-induced changes in amorphous hydrogenated carbon thin films. Diamond and Related Materials, 2013, 37, 97-103.	1.8	19

#	Article	lF	CITATIONS
19	Thermal stability and long term hydrogen/deuterium release from soft to hard amorphous carbon layers analyzed using in-situ Raman spectroscopy. Comparison with Tore Supra deposits. Thin Solid Films, 2015, 581, 92-98.	0.8	19
20	Investigating the Possible Origin of Raman Bands in Defective sp2/sp3 Carbons below 900 cmâ~1: Phonon Density of States or Double Resonance Mechanism at Play?. Journal of Carbon Research, 2019, 5, 79.	1.4	19
21	Time evolution of the ν2 IR absorption of (o-H2)n:H2O clusters (n=11–1), and increase of H2O rotation, in O2 doped solid hydrogen at 4.2K. Chemical Physics Letters, 2008, 454, 61-64.	1.2	18
22	Deuterium Inventory in Tore Supra: status of post-mortem analyses. Physica Scripta, 2009, T138, 014027.	1.2	18
23	Raman study of CFC tiles extracted from the toroidal pump limiter of Tore Supra. Journal of Nuclear Materials, 2011, 415, S254-S257.	1.3	16
24	Deuterium Inventory in Tore Supra (DITS): 2nd post-mortem analysis campaign and fuel retention in the gaps. Journal of Nuclear Materials, 2011, 415, S757-S760.	1.3	16
25	<i>In-situ</i> characterisation of the dynamics of a growing dust particle cloud in a direct-current argon glow discharge. Journal Physics D: Applied Physics, 2016, 49, 045203.	1.3	16
26	Formation of thin tungsten oxide layers: characterization and exposure to deuterium. Physica Scripta, 2016, T167, 014036.	1.2	16
27	Raman micro-spectroscopy as a tool to measure the absorption coefficient and the erosion rate of hydrogenated amorphous carbon films heat-treated under hydrogen bombardment. Diamond and Related Materials, 2012, 22, 92-95.	1.8	15
28	Hydrogen retention in beryllium: concentration effect and nanocrystalline growth. Journal of Physics Condensed Matter, 2015, 27, 475401.	0.7	15
29	The effect of beryllium oxide on retention in JET ITER-like wall tiles. Nuclear Materials and Energy, 2019, 19, 346-351.	0.6	15
30	Raman microscopy investigation of beryllium materials. Physica Scripta, 2016, T167, 014027.	1.2	14
31	Theoretical investigation on the point defect formation energies in beryllium and comparison with experiments. Nuclear Materials and Energy, 2017, 12, 453-457.	0.6	14
32	Simulation of the time dependent infrared ν2 mode absorptions of (oH2)n:H2O clusters in O2 doped solid hydrogen at 4.2K. Journal of Chemical Physics, 2009, 130, 054503.	1.2	13
33	Structure of the carbon layers deposited on the toroidal pump limiter of Tore Supra. Journal of Nuclear Materials, 2011, 415, S258-S261.	1.3	13
34	Erosion–deposition mapping of the toroidal pump limiter of Tore Supra. Journal of Nuclear Materials, 2013, 438, S771-S774.	1.3	13
35	Long-term H-release of hard and intermediate between hard and soft amorphous carbon evidenced by in situ Raman microscopy under isothermal heating. Diamond and Related Materials, 2013, 37, 92-96.	1.8	12
36	Modelling of the micrometric erosion pattern observed on the Tore Supra limiter tiles. Nuclear Fusion, 2014, 54, 123006.	1.6	12

C?DRIC PARDANAUD

#	Article	IF	CITATIONS
37	Inâ€plane and outâ€ofâ€plane defects of graphite bombarded by H, D and He investigated by atomic force and Raman microscopies. Journal of Raman Spectroscopy, 2015, 46, 256-265.	1.2	12
38	Effect of composition and surface characteristics on fuel retention in beryllium-containing co-deposited layers. Physica Scripta, 2020, T171, 014038.	1.2	12
39	Tungsten oxide thin film exposed to low energy He plasma: Evidence for a thermal enhancement of the erosion yield. Journal of Nuclear Materials, 2017, 484, 91-97.	1.3	11
40	Structural analysis of eroded carbon fiber composite tiles of Tore Supra: insights on ion transport and erosion parameters. Physica Scripta, 2011, T145, 014024.	1.2	10
41	Organic multishell isostructural host–guest crystals: fullerenes C60 inside a nitroxide open framework. Chemical Communications, 2013, 49, 3519.	2.2	10
42	Preparing the future post-mortem analysis of beryllium-based JET and ITER samples by multi-wavelengths Raman spectroscopy on implanted Be, and co-deposited Be. Nuclear Fusion, 2017, 57, 076035.	1.6	10
43	Post-mortem analysis of tungsten plasma facing components in tokamaks: Raman microscopy measurements on compact, porous oxide and nitride films and nanoparticles. Nuclear Fusion, 2020, 60, 086004.	1.6	10
44	Plasma-wall interaction studies in W7-X: main results from the recent divertor operations. Physica Scripta, 2021, 96, 124059.	1.2	10
45	Hydrogen in beryllium oxide investigated by DFT: on the relative stability of charged-state atomic versus molecular hydrogen. Journal of Physics Condensed Matter, 2018, 30, 305201.	0.7	8
46	Adsorption of Rhodamine 6G on SiO ₂ and Ag@SiO ₂ Porous Solids: Coupling Thermodynamics and Raman Spectroscopy. Journal of Physical Chemistry C, 2014, 118, 15308-15314.	1.5	7
47	Tungsten oxide thin film bombarded with a low energy He ion beam: evidence for a reduced erosion and W enrichment. Physica Scripta, 2017, T170, 014019.	1.2	7
48	Influence of magnetic field strength on nanoparticle growth in a capacitively-coupled radio-frequency Ar/C ₂ H ₂ discharge. Plasma Research Express, 2019, 1, 015012.	0.4	7
49	Simultaneous deuterium implantation and ion beam microanalyses in CFC NB31: Understanding the in-bulk migration. Journal of Nuclear Materials, 2013, 438, S975-S978.	1.3	6
50	Observation of methane nuclear spin isomers in gas phase at low temperature. Journal of Molecular Spectroscopy, 2012, 279, 37-43.	0.4	5
51	Raman microscopy as a defect microprobe for hydrogen bonding characterization in materials used in fusion applications. Physica Status Solidi C: Current Topics in Solid State Physics, 2015, 12, 98-101.	0.8	5
52	The role of defects, deuterium, and surface morphology on the optical response of beryllium. Nuclear Fusion, 0, , .	1.6	5
53	Contribution to a better evaluation of the dust speciation in case of an accident in ITER. Fusion Engineering and Design, 2017, 124, 1171-1176.	1.0	4
54	Forming Weakly Interacting Multilayers of Graphene Using Atomic Force Microscope Tip Scanning and Evidence of Competition between Inner and Outer Raman Scattering Processes Piloted by Structural Defects. Journal of Physical Chemistry Letters, 2019, 10, 3571-3579.	2.1	4

C?DRIC PARDANAUD

#	Article	IF	CITATIONS
55	Enhancing surface production of negative ions using nitrogen doped diamond in a deuterium plasma. Journal Physics D: Applied Physics, 2020, 53, 465204.	1.3	4
56	Multi-technique coupling for analysis of deuterium retention in carbon fiber composite NB31. Journal of Materials Science, 2015, 50, 7031-7042.	1.7	3
57	Formation of cyanide compounds during preparation of gold surfaces evidenced by surfaceâ€enhanced <scp>R</scp> aman spectroscopy. Journal of Raman Spectroscopy, 2018, 49, 1184-1189.	1.2	3
58	Single-crystal and polycrystalline diamond erosion studies in Pilot-PSI. Journal of Nuclear Materials, 2018, 500, 110-118.	1.3	3
59	Detection of Rhodamine 6G at low concentrations using Raman Spectroscopy: A comparison between Ag and Au-based nanoporous substrates. European Physical Journal: Special Topics, 2015, 224, 2001-2010.	1.2	2
60	Raman Microscopy: A Suitable Tool for Characterizing Surfaces in Interaction with Plasmas in the Field of Nuclear Fusion. , 2017, , .		2
61	Spectral fluctuation in SERS spectra of benzodiazepin molecules: The case of oxazepam. Journal of Raman Spectroscopy, 2020, 51, 2192-2198.	1.2	2
62	D retention and material defects probed using Raman microscopy in JET limiter samples and beryllium-based synthesized samples. Physica Scripta, 2021, 96, 124031.	1.2	2
63	Spectroscopic Measurements of Methane Solid–Gas Equilibrium Clapeyron Curve between 40 and 77 K. Journal of Physical Chemistry A, 2019, 123, 3518-3534.	1.1	1
64	Comparison of Nanoparticles Collected in the MAST Tokamak with Those Produced in Laboratory Plasmas. , 2011, , .		0
65	Plasma growth processes inside gaps of the castellated limiter of the Tore Supra tokamak. EPJ Applied Physics, 2011, 56, 24027.	0.3	0